



Intermolecular interaction studies of binary liquid mixtures of 2-methyl cyclohexanone with o-anisidine/m-anisidine/p-anisidine in terms of thermo-acoustic parameters at different temperatures

G Venkata Gangadhara Rao, Shaik Babu*, T Kalimulla & K Govind Rao
KoneruLakshmaiah Education Foundation, Physics Department (Guntur, Andhra Pradesh, India)

Received 8 April 2019; accepted 10 July 2020

In this present investigation, the thermo-acoustic fundamental parameters such as density (ρ) and speed of sound (U) were measured experimentally for the anisidine isomers (2-methoxy aniline, 3-methoxy aniline and 4-methoxy aniline) with solvent agent such as 2-methyl cyclohexanone in various concentrations within temperatures from 303.15 to 313.15K (5K interval) at ambient atmospheric pressure. From these experimentally determined values, various thermo-acoustic parameters of excess isentropic compressibility, K_s^E and excess molar volume, V_m^E are calculated. The calculated excess functions were correlated with reduced *Redlich-Kister* polynomial equation and results are analyzed in terms of structural molecular interactions between component molecules. Moreover, calibration of the partial molar volume's and partial isentropic compressibility's of components shows strong interaction in 2-methyl cyclohexanone + 4-methoxy aniline than any other composites. In addition to the FTIR characteristic spectrum of all combinations at different concentrations gives the more promising features such as interaction behavior that helps our analysis to guide the interactions of individual bonding strength of the molecules.

Keywords: anisidine isomers, *Redlich-Kister* functions, reduced *Redlich-Kister* functions, partial molar volumes, partial isentropic compressibilities, FT-IR spectrum.

Introduction

The unique features of molecular interactions in binary systems execute an imperative role in many industrial applications and contemporary investigations. In this association, the analysis of thermodynamic fundamental characteristics such as density and speed of sound on subsequent temperature intervals at ambient atmospheric pressure portrays the molecular interactions in binary systems. From these fundamental characteristics appraised the excess thermodynamic acoustic parameters regard to specific or non-specific interactions such as interaction strength, dipole inclusions and steric behavior of the molecules in the composites. Several research pioneers have been eclectically marked the intermolecular interactions of handful liquid mixtures with concern to excess thermodynamic acoustic parameters. In this experimental framework, methoxy and aniline wing aromatic nature of three isomers akin to 2-methoxy aniline (2MA), 3-methoxy aniline(3MA), 4-methoxy aniline(4MA) are independently blended with 2-methyl cyclohexanone

(2MCH). These isomers and their derivatives are mostly used in the prevention of corrosions of iron in oil refinery rigs¹. on the other hand the steric chair flip cycloalkane of 2MCH has been greatly used as solvent in many industrial and pharmaceutical sectors². Several pioneers³⁻⁶ eclectically researched the combination of aromatic aniline group with chiral cyclohexanone group. The present experimental work illustrates the multi component liquid mixtures of 2MA/3MA/ 4MA(1)+2MCH(2) at regular intervals of constant temperature from 303.15 to 313.15K over a constant ambient atmospheric pressure. In order to evaluate molecular interactions, the extracted excess values such as excess volume, V_m^E and excess isentropic compressibility, K_s^E has been fitted to the *Redlich-Kister* (RK) non-linear polynomial regression equation of the order four⁷. Since the non-ideality combination of aromatic aniline group with methyl group of cyclohexanone are highly reactive at low concentration. Hence, this approach sporadically misguides the specific interactions at low concentrations. In order to illustrate intermolecular hydrogen bonding nature and strength, the excess values are fitted to Reduced *Redlich-Kister* (RRK)

Corresponding author: (E-mail: babu.computers@gmail.com)

non-linear polynomial regression equation^{8,9}. Additionally, to promote extent of solvation behavior of composites partial molar volumes and partial isentropic compressibilities for composites have been conceived. The extracted results are reviewed on the basis of intermolecular interactions between component molecules with the help of FTIR spectrum, which is recorded at room temperature¹⁰.

Experimental courses

Materials description

In the present sequence, the provenance, CAS number, purity and further purification under chromatography and drying methods of anisidine isomers as well as 2MCH have been illustrated in Table-1. Further, the Table-2 illustrated the Purity of 2MA and 2MCH was gauged by comparison of experimental density and speed of sound with literature values. Furthermore, the unexplored density and speed of sound values of the 3MA and 4MA are propounded in the Table 2.

Evaluation methodology

The prepared binary mixtures and pure liquids were streamed in to glass vials with the help of mass

variations of liquids. The vials are covered with air tight lids in order to prevent evaporation and adsorption of atmospheric moisture. The uncertainty in the final mole fraction is estimated to be less than ± 0.0001 . The binary mixtures of systems such as 2MA(1)+2MCH(2), 3MA(1)+2MCH(2) and 4MA(1)+2MCH(2) were prepared in different concentrations, *i.e.*, molefractions of these systems carried out 12 subsequent values, on which solvation concentration varies from 0 to 1.

The densities of pure samples and mixed samples were measured with 10mL specific gravity bottle in high accuracy digital electronic balance supplied by *Mettler Toledo*, Company-India. The uncertainty weighing balance is approximated to be $\pm 10^{-8}$ gm leads to the accuracy in the densities is estimated to be less than $\pm 0.01 \text{ kg.m}^{-3}$.

The speed of sound measurements for the samples were performed by using with 2 MHz frequency single crystal ultrasonic interferometer supplied by *Nunes*, Company-India. The data accuracy in speed of sound is estimated to be less than $\pm 0.5 \text{ m.s}^{-1}$.

The parameters of all three systems were encapsulated with regular temperature intervals using

Table 1 – Specification of provenance, CAS number, mass fraction purity and further purification.

Name of the chemical	Source	CAS number	mass fraction purity	Further Purification Methods
2-methoxy aniline	TCI Chemicals-India	90-04-0	>98.0%	*GLPC
3-methoxy aniline	TCI Chemicals-India	536-90-3	>98.0%	*GLPC
4-methoxy aniline	TCI Chemicals-India	104-94-9	>98.0%	**Vacuum drying
2-methyl cyclohexanone	HiMedia Laboratories, India.	583-60-8	>99.70%	*GLPC

*Gas-Liquid Partition Chromatography carried through Inert gas Ar.
**moisture separation by mass transfer.

Table 2 – Physical properties of pure components of 2MCH, 2MA, 3MA & 4MA with literature at specific temperatures.

Sample	parameter	Exp./Lit.	Temperatures		
			303.15 K	308.15 K	313.15 K
2-methyl cyclohexanone	$\rho(\text{kg. m}^{-3})$	Expt.	920.80	911.22	907.45
	$\rho(\text{kg. m}^{-3})$	Lit.	920.84 ^a	911.20 ^a	907.44 ^a
	$U(\text{m.s}^{-1})$	Expt.	1346.00	1324.3	1303.2
	$U(\text{m.s}^{-1})$	Lit.	1346.00 ^a	1324.2 ^a	1303.8 ^a
2-methoxy aniline	$\rho(\text{kg. m}^{-3})$	Expt.	1091.80	1087.40	1083.80
	$\rho(\text{kg. m}^{-3})$	Lit.	1091.75 ^b	1087.35 ^b	1083.78 ^b
	$U(\text{m.s}^{-1})$	Expt.	1595.44	1579.44	1466.32
	$U(\text{m.s}^{-1})$	Lit.	1595.4 ^b	1579.2 ^b	1466.3 ^b
3-methoxy aniline	$\rho(\text{kg. m}^{-3})$	Expt.	1090.25	1087.05	1083.2
	$U(\text{m.s}^{-1})$	Expt.	1581.2	1550.32	1523.8
4-methoxy aniline	$\rho(\text{kg. m}^{-3})$	Expt.	1089.9	1085.2	1082.6
	$U(\text{m.s}^{-1})$	Expt.	1555.2	1525.4	1502.8

*The calibrated uncertainties are $U_c(\rho)=0.036\text{kg.m}^{-3}$, $U_c(U)=0.456\text{m.sec}^{-1}$, $U_c(x_1)=0.000037$, $U_c(T)=0.01\text{K}$ are carried at ambient atmospheric pressure. ^aReference[11] ^bReference[12]

a well stirred circulated water bath furnished by Nunes, Company-India, has been used to keep constant temperature within the accuracy of ± 0.01 K.

Results and discussions

The experimentally calibrated parameters of density ρ and speed of sound U over entire compositions of 2MA(1)+2MCH(2), 3MA(1)+2MCH(2) and 4MA(1)+2MCH(2) with temperature ranges 303.15K, 308.15K, 313.15 K are graphically illustrated in Fig. 1(a-c) and Fig. 2(a-c) respectively. The occurrent feature of all these attributes as regards to mole fraction shows non-linear increasing trend, and also shows reduction as regards to increasing temperature in entire compositions. The non-linear abnormalities of trends of these liquid components implies molecular interactions are exists between them³.

The excess thermodynamic acoustic parameters of binary solution have been esteemed with several peer reviewed journals. The eventual general expression was:

$$\gamma^E = \gamma^r - \gamma^{id} \quad \dots (1)$$

Here, $\gamma^E = V_m^E, K_s^E$ and $\gamma^r \{= V_m(\text{molar volume}), K_s(\text{isentropic compressibility})\}$ is the real value

of mixtures. And, the ideal component of thermodynamic acoustic parameters stands for

$$\gamma^{id} = x_1 Y_1 + (1 - x_1) Y_2 \quad \dots (2)$$

Here, x_1 is the molefraction of component of 2MA/3MA/4MA with respect to 2MCH. Y_1 and Y_2 are the pure acoustic values of 2MA/3MA/4MA and 2MCH respectively.

Redlich-Kister polynomial analysis

The conventional non-linear curve fitting strategy for attributes of binary mixture pertains *Redlich-Kister* polynomial regression⁷. The standard deviation was calibrated from the consequence

$$Y_{RK}^E = x_1(1 - x_1) \sum_{p=0}^{p=N} A_{p,T} (2x_1 - 1)^p \quad \dots (3)$$

Here, Y_{RK}^E means excess attribute of any value (*i.e.*, V_m^E, K_s^E) has been taken

$$\sigma(Y_{RK}^E) = \sqrt{\sum_{i=1}^{i=N} \frac{(Y_{i,exp} - Y_{i,cal})^2}{M - N}} \quad \dots (4)$$

Where M stands for the number of experimental values and N stands for the adjustable parameter. These excess values are examined with *Redlich-Kister* polynomial non-linear regression, and the values of

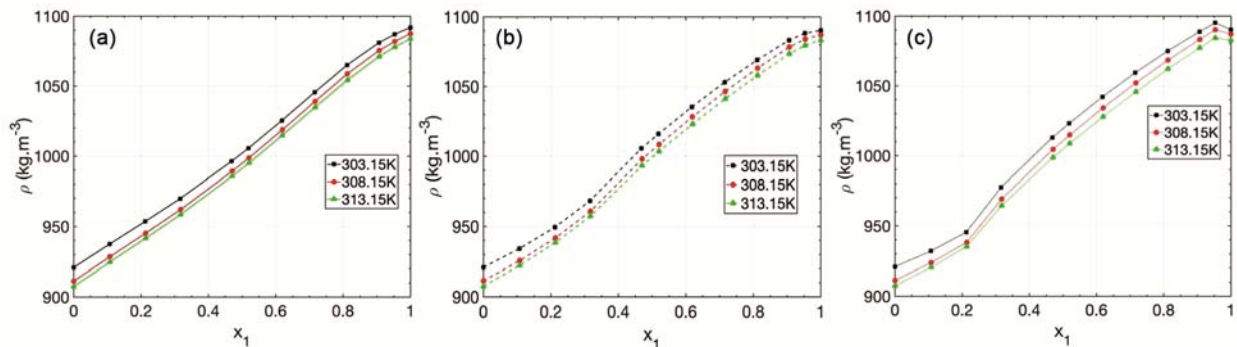


Fig. 1 – Density variation of composites with respect to molefraction (a)2MA(1)+2MCH(2) & (b)3MA(1)+2MCH(2)

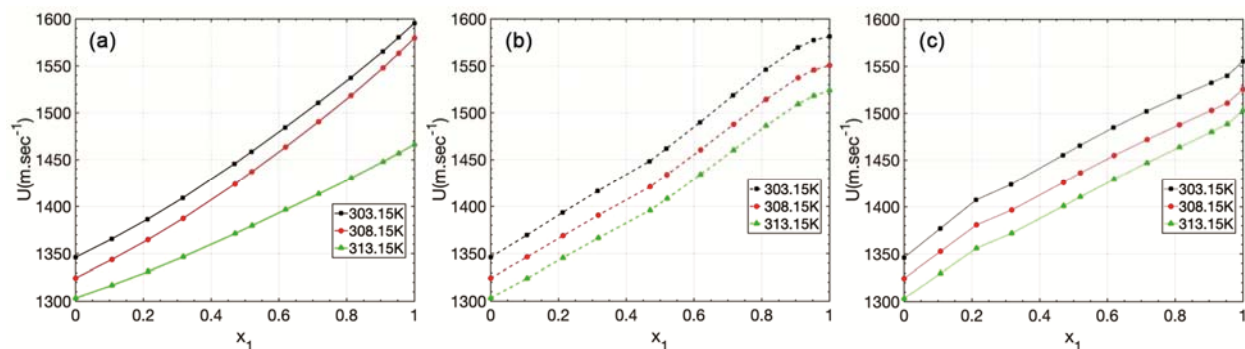


Fig. 2 – Speed of Sound variation of composites with respect to molefraction. (a)2MA(1)+2MCH(2) & (b)3MA(1)+2MCH(2)

$A_{i,T}$ ($i=0,1,2,3$) are determined along with standard deviation for experimental values and calibrated values. Table 3 catalogued the whole values of all composites.

The abnormality of thermodynamic acoustic excess parameters of V_m^E, K_s^E are portrayed in Figs 3-4 respectively. Due to thermal agitations of all composites, temperature rise ushers to descend the excess parameters. The abnormality of excess molar volume at all temperatures has been illustrated in Fig. 3 over an entire concentration for all composites. The values V_m^E are attributes positive for high concentrations of 2MCH and the trend turns to negative during the increasing concentration of 2MA, 3MA & 4MA in the respective composites.

The flipping sharpness of V_m^E from positive to negative was greater in 4MA(1)+2MCH(2) than compared to the other composites of 3MA(1)+2MCH(2)&2MA(1)+2MCH(2) respectively. This is clearly visible in Fig. 3, for the replicated sequence V_m^E . This clearly distinguishes the formation of H-bond¹¹,

which is stronger at higher concentration and weaker in lower concentrations of composites. In addition to that, formation of H-bond is very weak at high concentrations of MCH. The order of H-bond formation reactive in terms of V_m^E values are 4MA(1)+2MCH(2)>3MA(1)+2MCH(2)>2MA(1)+2MCH(2).

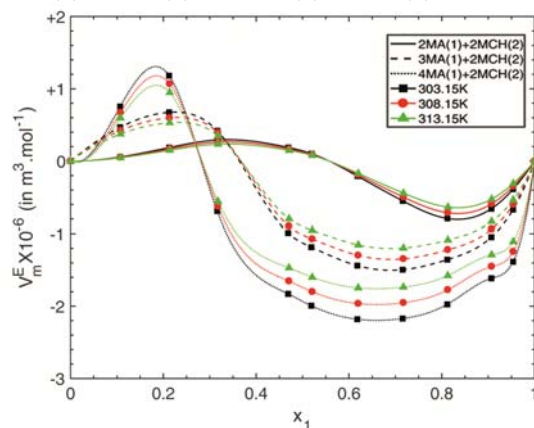


Fig. 3 – Excess Molar Volume variations against molefraction of solutions.

Table 3 – Coefficients of Redlich-Kister equation and standard deviations for excess parameters of various binary mixtures.

Combination	T/K	Redlich-kister equation coefficients				error $\sigma(V_{RK}^E)$
		$A_{0,T}$	$A_{1,T}$	$A_{2,T}$	$A_{3,T}$	
$V_m^E(10^{-6} \text{ m}^3.\text{mol}^{-1})$	303.15	0.5539	-4.3681	-6.3193	-1.0311	0.0254
2MA(1)+2MCH(2)	308.15	0.4977	-3.9161	-5.6926	-0.9524	0.0232
	313.15	0.4421	-3.4828	-5.0525	-0.8326	0.0217
	303.15	-28.2441	-30.2306	-12.1652	11.9465	4.7774×10^{-6}
$K_s^E(10^{-12} \text{ m}^2.\text{N}^{-1})$	308.15	-26.2670	-28.1145	-11.3136	11.1102	4.9272×10^{-6}
	313.15	-24.2900	-25.9985	-10.4620	10.2743	7.6317×10^{-6}
	303.15	-3.4285	-14.1873	0.6371	5.4831	0.0083
$V_m^E(10^{-6} \text{ m}^3.\text{mol}^{-1})$	308.15	-3.0379	-12.8841	0.4278	5.1367	0.0042
	313.15	-2.6956	-11.4540	0.3691	4.5710	0.0027
	303.15	-68.3669	-58.9428	-48.8878	-27.0333	0.0645
$K_s^E(10^{-12} \text{ m}^2.\text{N}^{-1})$	308.15	-63.3542	-55.0253	-46.1244	-25.7149	0.0621
	313.15	-58.5688	-50.8979	-42.7012	-23.8234	0.0576
	303.15	-7.3862	-9.0629	5.1022	-15.0198	0.1380
$V_m^E(10^{-6} \text{ m}^3.\text{mol}^{-1})$	308.15	-6.6310	-8.3842	4.4603	-13.0064	0.1348
	313.15	-5.8970	-7.4595	3.9733	-11.5507	0.1205
	303.15	-119.869	0.2157	26.3926	-0.5617	0.0028
$K_s^E(10^{-12} \text{ m}^2.\text{N}^{-1})$	308.15	-111.4786	0.2042	24.5479	-0.5319	0.0026
	313.15	-103.0877	0.1889	22.7002	-0.4919	0.0024

**The calibrated uncertainties are $U_c(V_m^E)=0.00024 \times 10^{-6} \text{ m}^3.\text{mol}^{-1}$, $U_c(K_s^E)=4 \times 10^{-16} \text{ m}^2.\text{N}^{-1}$ are carried at ambient atmospheric pressure.

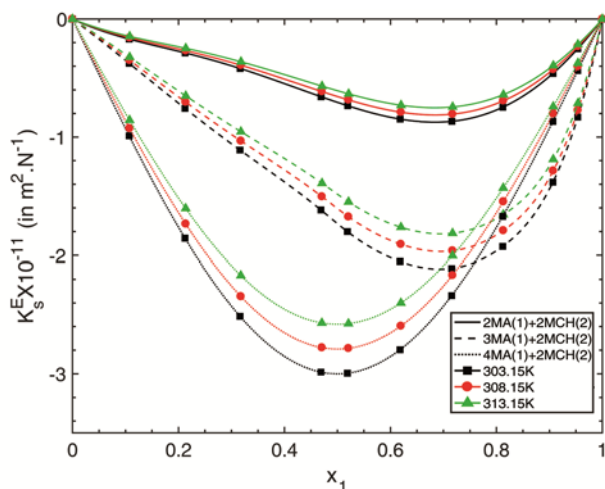


Fig. 4 – Excess isentropic compressibility variations against molefraction of solutions.

The abnormality of excess isentropic compressibility at all temperatures has been illustrated in Fig. 4 over an entire concentration for all composites. The K_s^E values are negative at all investigated temperatures for all composites. The sign of K_s^E plays a vital role in assessing the compactness due to molecular interactions in multi-component mixtures through electric charge transfer, dipole-dipole interactions, and dipole-induced dipole interactions in between bonds of successive constituent elements. It also suggests interstitial accommodation and oriental ordering leading to more compact structure making, which enhances K_s^E to negative values. Fort and Moore indicated that the binary liquids having distinct molecular sizes and shapes mix well there by reducing the volume which causes values of K_s^E to be negative. The K_s^E of negative was greater in 4MA(1)+2MCH(2) than compared to the other composites of 3MA(1)+2MCH(2)&2MA(1)+2MCH(2) respectively¹². This is clearly visible in Fig. 4. This clearly distinguishes a greater steric hindrance to the formation of hydrogen bonds in the respective composites. The order of K_s^E values are 4MA(1)+2MCH(2) > 3MA(1)+2MCH(2) > 2MA(1)+2MCH(2).

Reduced Redlich-Kister polynomial analysis

The ineluctable Redlich-Kister approach sporadically misguides the dissimilar composites. In conjunction to that it deceives interactions of molecules at low concentration regions in composites. Consequently, Desnoyers suggested a contemporary befitted *Reduced Redlich-Kister* (RRK) polynomial

analysis to address more specific features in composites¹³.

$$Q_{Y_{RK,T}^E}(x_1) = \frac{Y_{RK}^E(x_1)}{x_1(1-x_1)} \quad \dots (5)$$

The above specification is equivalent to apparent molar quantity of respective excess parameters in entire concentration ranges. Excess thermodynamic quantities have the convenience of showing the flipping sign, sharpness and magnitude of the dissimilarity composites, but the RRK polynomial specification elucidates a promising feature to lift the origin of the dissimilarity solutions¹⁴.

The reduced thermodynamic excess acoustic parameters of corresponding thermodynamic excess acoustic parameters have been illustrated in Table 4.

On applying the reduced function on V_m^E & K_s^E the graphs of Figs 3&4 turn in to Figs 5 & 6 respectively. The abnormality of $Q_{V_m^E,T}(x_1)$ at all temperatures has been illustrated in Fig. 5 over an entire concentration for all composites. The values $Q_{V_m^E,T}(x_1)$ are attributes positive (higher value) for high concentrations of 2MCH and the trend turns to negative (lower value) during the increasing concentration of 2MA, 3MA & 4MA in the respective composites. The decreasing trend of value from positive to negative was greater in 4MA(1)+2MCH(2) than compared to the other composites of 3MA(1)+2MCH(2)&2MA(1)+2MCH(2) respectively. This is clearly visible in Fig. 5, for the replicated sequence. This evidently distinguishes the hydrophobic interactions are present and stronger in the region of higher concentrations of methoxy aniline isomers¹⁵. In addition to that, Hydrophobic interactions are very weak at high concentrations of MCH. The order of interactions in terms of values are 4MA(1)+2MCH(2) > 3MA(1)+2MCH(2) > 2MA(1)+2MCH(2).

For the present scenario, the reduced functions values $Q_{K_s^E,T}(x_1)$ are higher value on 2MCH side and low value on 2MA/3MA/4MA side. This clearly visible in Fig. 5, for the replicated sequence of $Q_{K_s^E,T}(x_1)$. This result indicates composites are less compressible than the corresponding ideal mixtures. This is strongly evident that strong interactions occur in these composites. Here, higher concentration of 2MA/3MA/4MA side 3MA corresponding combination poses high negative values than any other combinations. This clearly indicates that the combination 3MA(1)

Table 4 – Coefficients of Reduced Redlich-Kister equation for excess parameters of various binary mixtures.

x_1	$Q_{V,T}^E(x_1)^*$ 10^{-6}	$Q_{K_S,T}^E(x_1)^*$ 10^{-10}	x_1	$Q_{V,T}^E(x_1)^*$ 10^{-6}	$Q_{K_S,T}^E(x_1)^*$ 10^{-10}	x_1	$Q_{V,T}^E(x_1)^*$ 10^{-6}	$Q_{K_S,T}^E(x_1)^*$ 10^{-10}
(2MA(1)+2MCH(2)) 303.15K			(2MA(1)+2MCH(2)) 308.15K			(2MA(1)+2MCH(2)) 313.15K		
0	-0.3273	-0.2213	0	-0.2887	-0.2058	0	-0.256	-0.1903
0.1071	0.5953	-0.178	0.1078	0.5358	-0.1654	0.1078	0.4762	-0.1529
0.2126	1.1145	-0.1716	0.2137	1.0017	-0.1596	0.2138	0.8902	-0.1476
0.3164	1.3541	-0.1938	0.3178	1.2136	-0.1806	0.318	1.0782	-0.1671
0.4691	0.7543	-0.2643	0.4707	0.667	-0.2466	0.4709	0.5915	-0.2282
0.5192	0.4087	-0.2942	0.5208	0.3518	-0.2746	0.521	0.3109	-0.254
0.6183	-0.8834	-0.3592	0.6198	-0.8147	-0.335	0.62	-0.7265	-0.3099
0.7159	-2.7103	-0.426	0.7172	-2.4602	-0.397	0.7174	-2.1893	-0.3673
0.812	-5.203	-0.4894	0.813	-4.7048	-0.4558	0.8131	-4.1845	-0.4215
0.9067	-7.7898	-0.5445	0.9073	-7.0382	-0.5067	0.9073	-6.2593	-0.4686
0.9535	-8.7762	-0.5676	0.9538	-7.9346	-0.528	0.9539	-7.0572	-0.4882
1	-11.3543	-0.5869	1	-10.243	-0.5458	1	-9.1076	-0.5048
(3MA(1)+2MCH(2)) 303.15K			(3MA(1)+2MCH(2)) 308.15K			(3MA(1)+2MCH(2)) 313.15K		
0	5.8829	-0.3128	0	5.1065	-0.2874	0	4.526	-0.2655
0.107	4.8961	-0.3931	0.1077	4.3938	-0.3634	0.1078	3.9047	-0.3359
0.2124	4.0312	-0.4526	0.2136	3.5553	-0.4191	0.2137	3.1551	-0.3874
0.3161	1.9421	-0.5134	0.3177	1.8126	-0.4761	0.3179	1.6157	-0.4402
0.4687	-3.9715	-0.6493	0.4706	-3.6016	-0.6036	0.4708	-3.2033	-0.5582
0.5189	-4.7396	-0.7213	0.5208	-4.2905	-0.671	0.5209	-3.8155	-0.6205
0.618	-6.0915	-0.8686	0.6198	-5.503	-0.8093	0.6199	-4.8931	-0.7485
0.7156	-7.3471	-1.0365	0.7171	-6.6309	-0.9671	0.7173	-5.8954	-0.8946
0.8118	-8.8728	-1.2605	0.813	-8.0233	-1.1778	0.813	-7.1345	-1.0895
0.9066	-12.3437	-1.6317	0.9072	-11.1502	-1.5269	0.9073	-9.9141	-1.4126
0.9535	-15.1442	-1.8719	0.9538	-13.698	-1.7529	0.9538	-12.1808	-1.6218
1	-11.4789	-2.0323	1	-10.3402	-1.9022	1	-9.1923	-1.7599
(4MA(1)+2MCH(2)) 303.15K			(4MA(1)+2MCH(2)) 308.15K			(4MA(1)+2MCH(2)) 313.15K		
0	21.7624	-0.9313	0	19.2185	-0.866	0	17.0812	-0.8008
0.107	7.9019	-1.0356	0.1077	6.9737	-0.9637	0.1077	6.1981	-0.8911
0.2124	7.0637	-1.1098	0.2136	6.358	-1.0328	0.2136	5.6515	-0.9551
0.3161	-3.1945	-1.1625	0.3177	-2.8924	-1.0817	0.3177	-2.5711	-1.0003
0.4687	-7.3456	-1.1989	0.4706	-6.6333	-1.1151	0.4706	-5.8963	-1.0312
0.5189	-7.9877	-1.1996	0.5208	-7.2103	-1.1156	0.5208	-6.4092	-1.0316
0.618	-9.2357	-1.1845	0.6198	-8.333	-1.1011	0.6198	-7.4073	-1.0182
0.7156	-10.6645	-1.1487	0.7171	-9.6219	-1.0676	0.7172	-8.553	-0.9872
0.8118	-12.9166	-1.0945	0.813	-11.6597	-1.0172	0.813	-10.3643	-0.9406
0.9066	-19.0587	-1.0247	0.9072	-17.2275	-0.9525	0.9072	-15.3138	-0.8808
0.9535	-31.2007	-0.985	0.9538	-28.2383	-0.9157	0.9538	-25.1015	-0.8468
1	-26.316	-0.9382	1	-23.5544	-0.8726	1	-20.9366	-0.8069

*** The values in parenthesis are extrapolated with 4th degree of RRK polynomial non-linear equation.

+2MCH(2) sterically hindered higher than any other combinations.

Partial molar volumes and partial isentropic compressibilities

The RRK functions of $Q_{V_m^E,T}(x_1)$ and $Q_{K_S^E,T}(x_1)$ at infinite dilution over a constant temperature and pressure was an addition tool to represents partial molar volumes and partial isentropic compressibilities at infinite dilutions. The above extrapolation expression³ has modified as:

$$Q_{V_m^E,T}(x_1=0)=A_{0,T}-A_{1,T}+A_{2,T}-A_{3,T}=\bar{V}_{1,p,m}^{E,\infty}=\bar{V}_{1,p,m}^{\infty}-V_{1,m} \quad \dots (6)$$

$$Q_{V_m^E,T}(x_1=1)=A_{0,T}+A_{1,T}+A_{2,T}+A_{3,T}=\bar{V}_{2,p,m}^{E,\infty}=\bar{V}_{2,p,m}^{\infty}-V_{2,m} \quad \dots (7)$$

$\bar{V}_{1,p,m}^{E,\infty}$ and $\bar{V}_{2,p,m}^{E,\infty}$ are excess partial molar volumes two pure components at infinite dilutions. $\bar{V}_{1,p,m}^{\infty}$ and $\bar{V}_{2,p,m}^{\infty}$ are partial molar volumes at infinite dilutions. $V_{1,m}$ and $V_{2,m}$ are pure molar volumes of

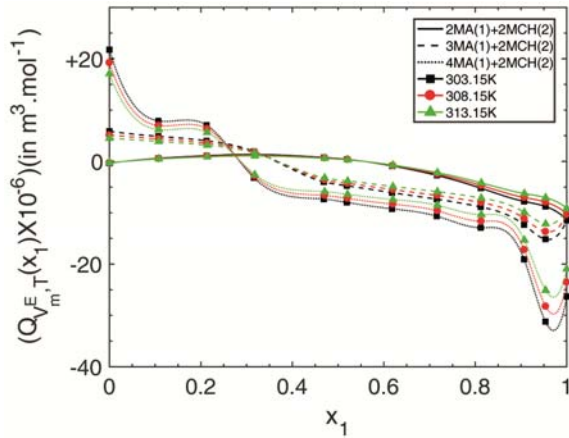


Fig. 5 – Reduced Excess Volume variations against molefraction of solutions.

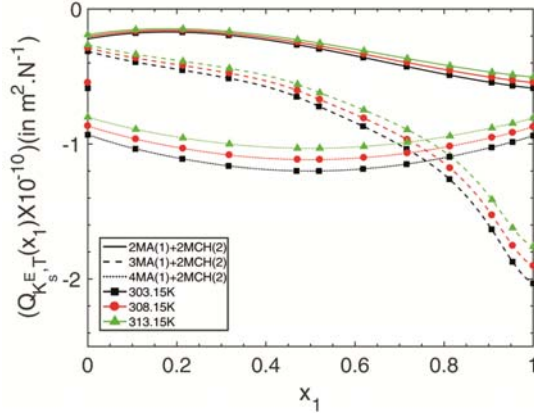


Fig. 6 – Reduced Excess Isentropic compressibility variations against molefraction of solutions.

two components 2MA/3MA/4MA and 2MCH. Similarly, the equation analogy is also true for partial isentropic compressibilities. But, the real-time analysis of partial molar volumes and partial isentropic compressibilities over a molefraction concentration at constant pressure and temperature can be evaluated from the differential equation is^{169,17}

$$\bar{V}_{i,p,m} = V_m(x_i) - x_j \left(\frac{\partial V_m(x_j)}{\partial x_j} \right)_{T,P} \quad \dots (8)$$

$$\bar{K}_{i,p,s} = K_s(x_i) - x_j \left(\frac{\partial K_s(x_j)}{\partial x_j} \right)_{T,P} \quad \dots (9)$$

Here x_i and x_j are the mole fractions of two components in the composite ($i=1,2$ & $j=i-1$). The intermolecular interactions in the composites can be interpreted in terms of packing efficiency of molecules with the help of partial molar volumes and partial isentropic compressibilities.

The partial molar volumes of two components $\bar{V}_{1,p,m}$ and $\bar{V}_{2,p,m}$ are playing vital role in binary mixture. Because the domain influence of the

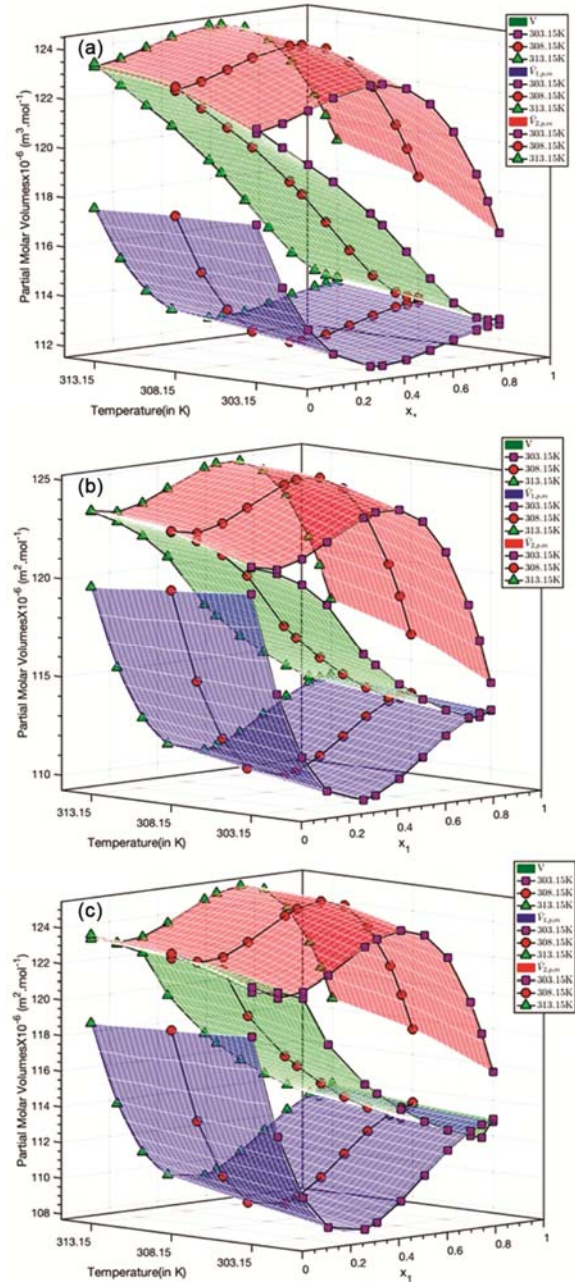


Fig. 7 – Plot of partial molar volumes against molefraction for the solutions 2MA(1)+2MCH(2), 3MA(1)+2MCH(2) & 4MA(1)+2MCH(2) at studied range of temperatures 303.15K, 308.15K & 313.15K.

components in the mixture changes with respect to the composition concentration and temperature. In this scenario, the partial molar volumes of components 2MA(1)+2MCH(2), 3MA(1)+2MCH(2) & 4MA(1)+2MCH(2) at all temperatures has been shelled in Fig. 7(a-c) respectively. In each of the figure, the mirror scaffolded Z symbol graph contains three colored meshes, which are concerned to blue

($\bar{V}_{1,p,m}$), green (total molar volume, V) and red ($\bar{V}_{2,p,m}$). For all combinations, the partial molar volumes of both components $\bar{V}_{1,p,m}$ and $\bar{V}_{2,p,m}$ are lower than of their individual values in the pure state, which reveals the domain influence of the individual components decreasing with their respective lower concentration regions¹⁸. The abnormality is examined for all constant intervals of temperatures. This clearly suggests presence of solute-solvent interactions in between unlike molecules. Hence, from the representation of Fig. 7(a-c), the effect of domain influence of volume is low for 4MA(1)+2MCH(2) than compared to the other composites of 3MA(1)+2MCH(2) & 4MA(1)+2MCH(2) respectively. This clearly suggests about, the solute-solvent interactions between molecules is high for 4MA(1)+2MCH(2) than compared to the other composites of 3MA(1)+2MCH(2) & 2MA(1)+2MCH(2).

The partial isentropic compressibilities of two components $\bar{K}_{1,p,s}$ and $\bar{K}_{2,p,s}$ are also play crucial role in binary mixture. Because the geometrical influence of the components in the mixture changes with respect to the composition concentration and temperature. In this scenario, the partial isentropic compressibilities of components 2MA(1)+2MCH(2), 3MA(1)+2MCH(2) & 4MA(1)+2MCH(2) at all temperatures has been shelled in Fig. 8(a-c) respectively. In each of the figure, the mirror scaffolded Z symbol graph contains three colored meshes, which are concerned to blue ($\bar{K}_{1,p,s}$), green (total isentropic compressibility, K_s) and red ($\bar{K}_{2,p,s}$). The partial isentropic compressibilities $\bar{K}_{1,p,s}$ and $\bar{K}_{2,p,s}$ are unchanged, negative and positive for the respective combinations of 2MA(1)+2MCH(2), 3MA(1)+2MCH(2) & 4MA(1)+2MCH(2). This reveals the geometrical compressibility influence of the individual components increasing with their respective lower concentration regions in 4MA(1)+2MCH(2) combination¹⁸. The abnormality is examined for all constant intervals of temperatures. This clearly suggests the strong dipole inclusions between 4MA(1)+2MCH(2) than compared to the other combinations of 3MA(1)+2MCH(2) & 2MA(1)+2MCH(2). Hence, from the representation of Fig. 8(a-c), the effect of geometrical influence is high for 4MA(1)+2MCH(2) than compared to the other composites of 3MA(1)+2MCH(2) & PA(1)+2MCH(2).

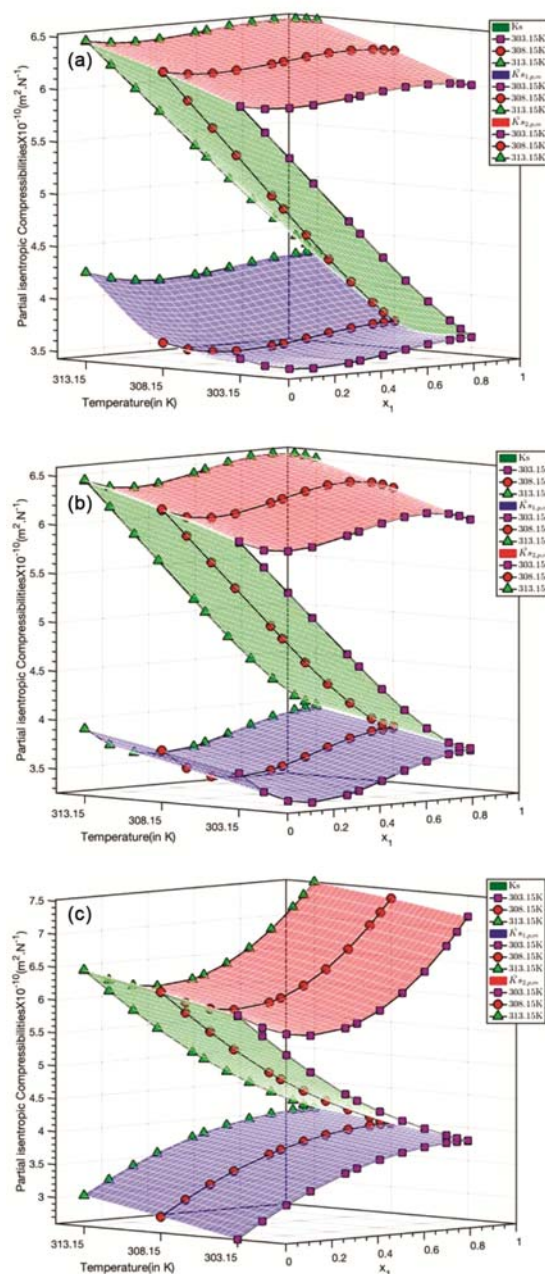


Fig. 8 – Plot of partial isentropic compressibilities against molefraction for the solutions 2MA(1)+2MCH(2), 3MA(1)+2MCH(2) & 4MA(1)+2MCH(2) at studied range of temperatures 303.15K, 308.15K & 313.15K.

FT-IR spectrum analysis

The FT-IR spectrum of components 2MA+2MCH, 3MA+2MCH & 4MA+2MCH and their pure components are carried at room temperature 303.15K. The peaks of intensity of 3438.79 cm^{-1} (N-H strong bond stretching), 3361.17 cm^{-1} (O-H strong bond stretching), 2934.73 cm^{-1} (C-H medium stretching) and 1706.10 cm^{-1} (C=O strong stretching) for the

combination 4MA+2MCH is stronger than 3MA+2MCH & 2MA+2MCH. This contention was supported by the formation of intermolecular strong bonds in respective combinations. The detail information of FTIR Spectrum of components are portrayed in Figure 9(a-c) and the monumental values are catalogued in Table 5¹⁰.

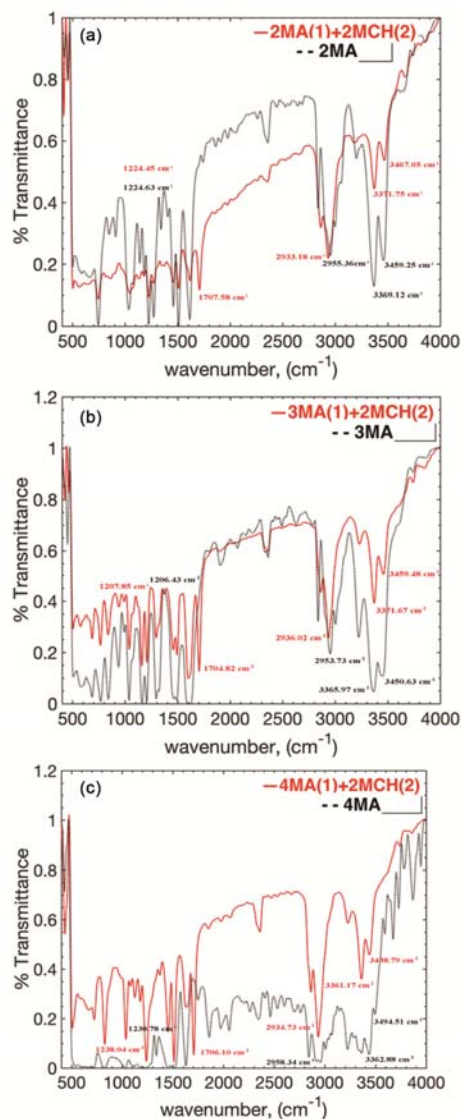


Fig. 9 – Normalized FT-IR spectra analysis for the binary mixtures over the range 400 to 4000 cm⁻¹ (a)2MA(1)+2MCH(2) versus 2MA & (b)3MA(1)+2MCH(2) versus 3MA

Conclusions

In this frame work, the values of excess thermodynamic parameters have been calibrated for an entire composition of 2MA(1)+2MCH(2), 3MA(1)+2MCH(2) & 4MA(1)+2MCH(2)with accustomed levels of temperatures. This is clearly elucidating a strong hydrogen bonding, dipole-inclusion interactions present in the component molecules. Moreover, the reduced excess thermodynamic parameters have been executed by using contemporary RRK polynomial over an entire composition with accustomed levels of temperatures. This reveals more specific features about, smaller molar mass of 2MCH molecules sterically hindered in larger molar mass of 2MA, 3MA &4MA in their respective compositions. The reduced excess parameters value decreases for increases of temperatures in their compositions due to their thermal agitations. The reactive of composites are in the order 2MA(1)+2MCH(2) <3MA(1)+2MCH(2)<4MA(1)+2MCH(2). Further, an addition tool partial molar volume was extracted from RRK polynomial. In this connection, the partial molar volumes of both components have been plotted in 3D graphs. This discloses the intermolecular interactions are strong in 4MA(1)+2MCH(2) composition compared to 3MA(1)+2MCH(2) & 2MA(1)+2MCH(2). These results of intermolecular interaction behavior also supported with FT-IR spectroscopy.

Disclosure statement

No potential conflict of interest was reported by the authors.

Acknowledgement

One of the authors (Dr. Shaik.Babu) would like to thank Department of Science and Technology (DST), Govt. of India, for the award of DST-FIST Level-1 (SR/FST/PS-1/2018/35) scheme to Department of Physics, KLEF. Author, G Venkata Gangadhara Rao is thankful to Dr.Shaik Babu, Department of Physics,

Table 5 – FT-IR analysis

Name of the component	N-H str cm ⁻¹	N-H str cm ⁻¹	C-H med cm ⁻¹	C-Nstr cm ⁻¹	C=O str cm ⁻¹	O-H str (H-bonded) cm ⁻¹
2MA	3459.25	3369.12	2955.36	1224.63	----	----
2MA+2MCH	3467.05	----	2933.18	1224.45	1707.58	3371.75
3MA	3450.63	3365.97	2953.73	1206.43	----	----
3MA+2MCH	3459.48	----	2936.02	1207.85	1704.82	3371.67
4MA	3494.51	3362.88	2958.34	1230.78	----	----
4MA+2MCH	3438.79	----	2934.73	1238.04	1706.10	3361.17

KLEF, Guntur for his valuable suggestions and discussions.

References

- 1 Haldar N, Shukla H S & Udayabhanu G, *Indian J Chem Technol*, 19 (2012) 173.
- 2 Jacolot M, Jean M, Levoine N & Weghe P van de, *Org Lett*, 14 (2012) 58.
- 3 Sreehari S S, Babu S, Vishwam T & Sie T H, *J Chem Thermodyn*, 68 (2014) 183.
- 4 Sastry S S, Babu S, Vishwam T & Tiong H S, *J Therm Anal Calorim*, 116 (2014) 923.
- 5 Rao K G, Kiran M G, Babu S & Santos D, *J Pharm Sci Res*, 9 (2017) 624.
- 6 Sreehari S S, Babu S, Vishwam T, Parvateesam K & Sie T H, *Physica B: Condens Matter*, 420 (2013) 40.
- 7 Redlich O & Kister A T, *Ind Eng Chem*, 40 (1948) 345.
- 8 Das D, Messaâdi A, Dhouibi N & Ouerfelli N, *Phys Chem Liq*, 50 (2012) 773.
- 9 Trabelsi R, Babu S, Salhi H, Ouerfelli N & Toumi A, *Phys Chem Liq*, 56 (2017) 801.
- 10 Balaji R, Gowri S M & Chandra S M, *J Mol Liq*, 216 (2016) 330.
- 11 Sankar M G, Ponneri V, Kumar K S & Sakamuri S, *J Therm Anal Calorim*, 115 (2014) 1821.
- 12 Mukesh B, Gowri Sankar M, Chandra S M & Srikanth T, *J Soution Chem*, 44 (2015) 2267.
- 13 Sastry S S, Babu S, Vishwam T & Ha S T, *Phys Chem Liq*, 52 (2014) 272.
- 14 Sastry S S, Ibrahim S M, Kumar L T, Babu S & Tiong H S, *Int J Eng Res Technol*, 4 (2015) 315.
- 15 Salhi H *et al.*, *Mediterranean J Chem*, 6 (2017) 33.
- 16 Salhi H *et al.*, *Rasyan J Chem*, 9 (2016) 864.
- 17 Nayeem S M, Nyamathulla S, Khan I & Rao D K, *J Mol Liq*, 218 (2016) 676.
- 18 Nagababu P, Babu S, D F S & M G, *Phys Chem Liq*, (2018).
- 19 Gardas R L, Dagade D H, Terdale S S, Coutinho J A P & Patil K J, *J Chem Thermodyn*, 40 (2008) 695.
- 20 Srinivasa R V, Vijaya K T, Madhu M T & Madhusudana R P, *J Chem Thermodyn*, 104 (2017) 150.